Brief Communication

Highlight article

Functional intrinsic optical signal imaging for objective optoretinography of human photoreceptors

Taeyoon Son[1] ⓘ **, Tae-Hoon Kim[1]** ⓘ **, Guangying Ma[1], Hoonsup Kim[1] and Xincheng Yao[1,2]**

[1]Department of Bioengineering, University of Illinois at Chicago, Chicago, IL 60607, USA; [2]Department of Ophthalmology and Visual Sciences, University of Illinois at Chicago, Chicago, IL 60612, USA
Corresponding author: Xincheng Yao. Email: xcy@uic.edu

Impact statement

Age-related macular degeneration and retinitis pigmentosa are known to cause phototransduction abnormalities in retinal photoreceptors. Fast intrinsic optical signal (IOS), due to transient outer segment changes correlated with phototransduction activation, promises one objective methodology for non-invasive mapping of photoreceptor function. We report here the feasibility of non-mydriatic IOS imaging for objective optoretinography of retinal photoreceptors in awake human.

Abstract

Functional mapping of photoreceptor physiology is important for better disease diagnosis and treatment assessment. Fast intrinsic optical signal (IOS), which arises before light-evoked pupillary response, promises a unique biomarker of photoreceptor physiology for objective optoretinography with high resolution. This study is to test the feasibility of non-mydriatic IOS mapping of retinal photoreceptors in awake human. Depth-resolved optical coherence tomography verified outer segment (OS) as the anatomic origin of fast photoreceptor-IOS. Dynamic IOS changes are primarily confined at OS boundaries connected with inner segment and retinal pigment epithelium, supporting transient OS shrinkage due to phototransduction process as the mechanism of the fast photoreceptor-IOS response.

Introduction

Retinal photoreceptors play an important role in phototransduction process which converts light energy into electrochemical signal for visual information processing. Phototransduction abnormalities have been demonstrated in diabetic retinopathy,[1,2] retinitis pigmentosa,[3,4] age-related macular degeneration,[5,6] etc. Early detection of photoreceptor dysfunctions is one essential step to enable prompt interventions for preventing irreversible vision loss. Traditional fundus photography can give useful information for eye examination, but the morphological only information is not sufficient.[7] In general speaking, physiological abnormality might appear in diseased cells before morphological deformations, such as retinal thickness change and cell loss. Therefore, functional assessment of physiological changes in retinal photoreceptor is important for early eye disease diagnosis. Electroretinography (ERG), including focal ERG[8–12] and multifocal ERG,[13,14] allows objective assessment of retinal physiological function. Particularly ERG a-wave provides an objective biomarker for assessing photoreceptor function. However, spatial resolution of ERG measurements is typically low. At early stages, eye diseases caused by

cellular damages are typically in the format of degenerative and apoptotic abnormalities of small groups of retinal neural cells. Thus, it is desirable to have a high-resolution method for objective measurement of physiological function of retinal photoreceptors.

Intrinsic signal imaging, which is also known as optophysiology or optoretinography (ORG),[15] can provide an objective method for mapping retinal physiology with high resolution.[16,17] In comparison with ERG that measure light-evoked electrophysiological activities, the ORG records transient intrinsic optical signal (IOS) changes in the retina. Light-evoked IOS changes were first reported in outer segment (OS) suspensions of photoreceptor[18–20] and isolated retinas.[21–23] These early studies showed that the transient IOS changes were closely related with early phase of the phototransduction. Recently, activation phase of phototransduction in retinal photoreceptors has been demonstrated in intact animal retinas, and photoreceptor-IOS abnormality has been also disclosed in mouse models with retinal degeneration.[24,25] Almost immediate arise of the photoreceptor-IOS after the stimulus onset can be a unique biomarker of objective ORG to assess retinal photoreceptor physiology.[26]

In vivo IOS imaging of human subjects has several technical challenges. First, the visible light can produce a pupillary response, and thus contaminate the IOS recording. Light-induced pupil constriction can reduce the pupil size and also increase focus depth of the ocular optics to affect optical coherence tomography (OCT) imaging. Since IOS imaging compares OCT recordings before and after the light stimulation, pupillary response may cause IOS artifact. In principle, pharmacological pupil dilation can minimize the effect of pupillary response. However, pharmacological pupil dilation is uncomfortable for the patients and may create extra complications, making the measurement time- and cost-consuming. Second, light-evoked neural activities at the inner retina and corresponding hemodynamic changes may contaminate the IOS recording of retinal photoreceptors. Fortunately, the rapid photoreceptor-IOS shows immediate onset after the stimulus, while an inner retina and hemodynamic changes have a time delay.[27–29] Previous studies revealed a ~0.5 s time delay of IOS changes at the inner retina,[28] and hemodynamic contamination can be compensated by digital vessel filtering.[27] Moreover, functional OCT can provide depth-resolved imaging capability to dissect the IOS changes at different retinal layers.[30–33] In the mouse retina, the fast photoreceptor-IOS can reach a magnitude peak within 20–30 ms.[28] We speculate that the fast photoreceptor-IOS in the human retina may have a similar time course as that in the mouse retina. If so, a 100 ms post-stimulus window can be enough for functional IOS imaging of retinal photoreceptors, which excludes the requirement of pupillary dilation because the pupil response typically occurs around ~300 ms after the visible light stimulus.[34]

In this study, we validate the feasibility of non-mydriatic IOS imaging for objective ORG of retinal photoreceptors in awake human and establish the spatiotemporal characteristics of the retinal transient IOS changes.

Materials and methods

The study has been approved by the Institutional Review Board at University of Illinois at Chicago and followed the tenets of the Declaration of Helsinki. Three healthy subjects (three men, mean age 31.67 ± 1.53 years) without history of ophthalmic disease were recruited for technical validation of functional IOS imaging of retinal photoreceptors. Each subject provided informed consent prior to participation in the research.

A lab-built functional OCT was employed for this study (Figure 1(a)). One NIR superluminescent diode (D-840-HP-I, Superlum, Cork, Ireland) was used in the OCT for NIR IOS imaging, while a visible light LED was used as the retinal stimulator. The illumination power was ~600 μW on the cornea for OCT imaging, which is below the American National Standards Institute limit. The axial and lateral pixel resolutions were calculated as 1.5 and 5.0 μm, respectively. For aiding retinal localization, a pupil camera was used, and to verify the time course of pupillary response (Figure 1(b)), corresponding to the retinal stimulation. A dim red light was used as fixation target to minimize voluntary eye movements. The OCT spectrometer was designed with a line-scan CCD camera which has a 70,000 Hz line rate and 2048 pixels. For the OCT imaging, the recording speed was 100 B-scan/s, with frame resolution of 500 A-lines/B-Scan. For the functional IOS imaging, the subjects were dark adapted for 1 h and then imaged at the fovea for 1.2 s. After the 0.2 s prestimulus, a 50 μW visible stimulus flash was applied to the adapted retina with a cold white LED (MCWHF1, Thorlabs, New Jersey).

Results

Figure 2 is representative OCT-IOS imaging. Basic procedures of IOS data processing have been reported in previous publications.[29] In order to minimize the effect of pupillary response on the IOS imaging, each pixel intensity was normalized relative to the inner retina, i.e. the inner plexiform layer, before IOS processing. Ten OCT and IOS images were averaged for Figure 2(a)–(c) and the raw recording speed was 100 B-scan/s. Figure 2(d) represents single frame recordings at different time points. Both positive (red) and negative (green) IOSs were observed (Figure 2(b)), which is consistent with our previous observation in animal retinas.[35] In order to simplify the discussion,
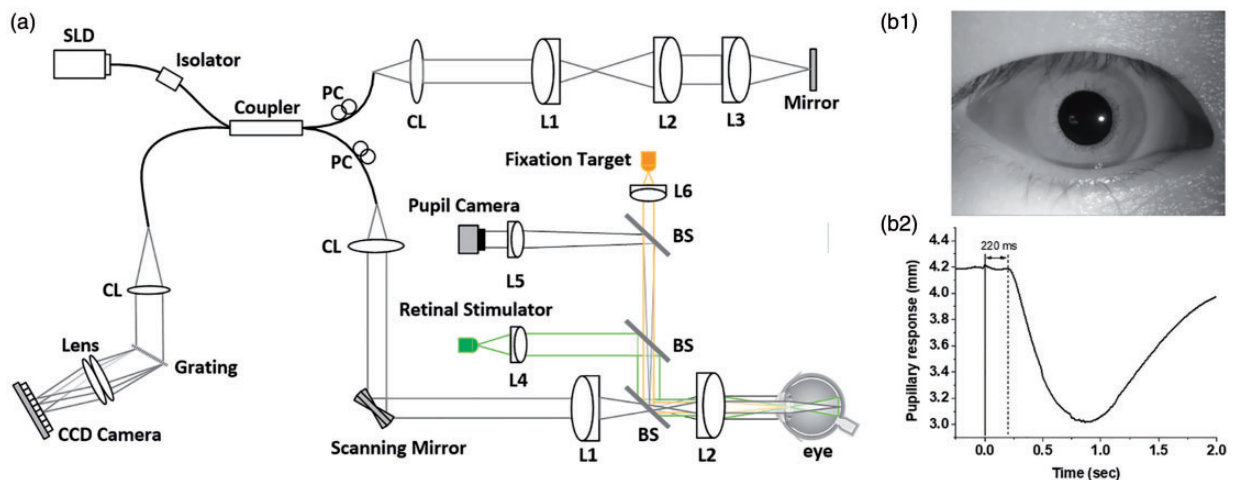
Figure 1. (a) Schematic diagram of the OCT system. BS: beam splitter; CL: collimation lens; Lenses: L1, L2, L3, L4, L5, and L6; PC: polarization controller; SLD: superluminescent diode. (b) Representative pupil image (b1) and pupillary response (b2). (A color version of this figure is available in the online journal.)
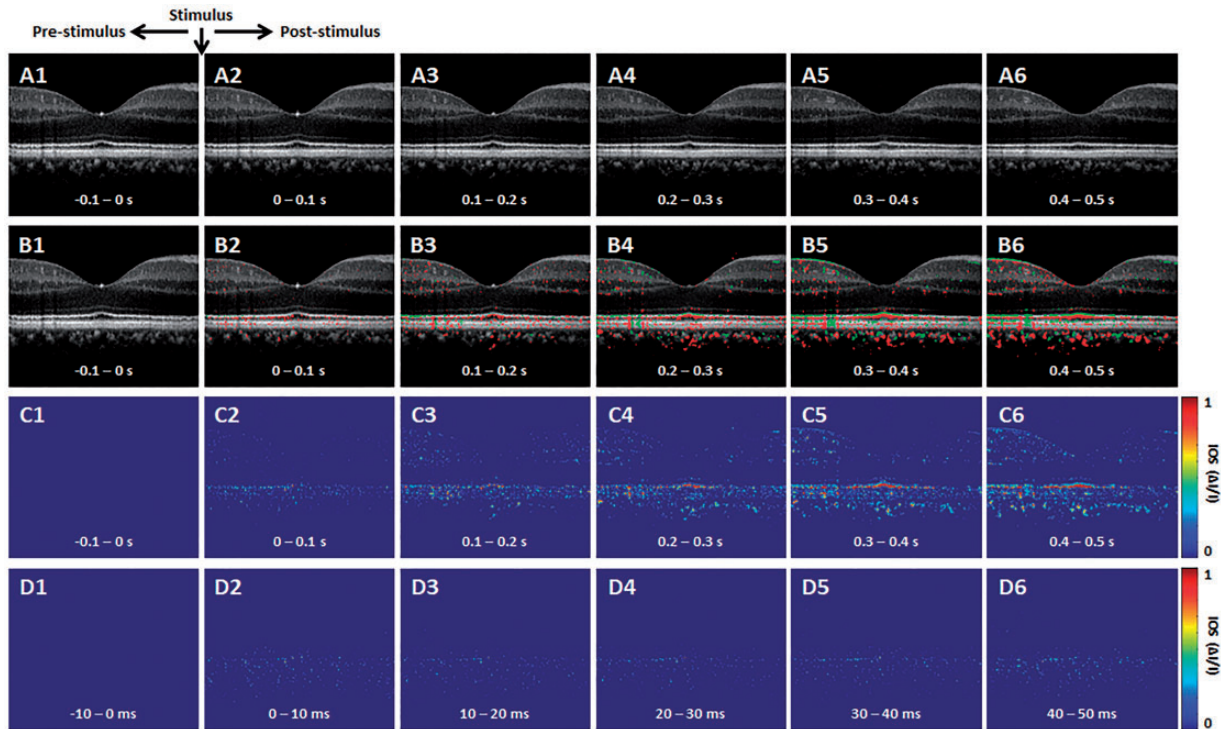
Figure 2. Representative OCT-IOS image sequence. (a) Representative OCT image sequence. (b) Corresponding IOS distributions of positive (red) and negative (green) changes. (c) IOS magnitude sequence with 0.1 s time intervals. (d) IOS magnitude sequence with 10 ms time intervals. (A color version of this figure is available in the online journal.)

we ignore the signal polarities to employ IOS magnitude values for following analysis of IOS time course and spatial distribution. As shown in Figure 2(b)–(d), rapid photoreceptor-IOSs occur promptly after the onset of stimulus. Particularly, for the first ~100 ms after-stimulus recording period, the IOS is primarily observed within the OS region. This is consistent with our previous animal study of fast photoreceptor-IOS.[30] Later IOS recording might be contaminated by corresponding pupillary response and hemodynamic change. However, as shown in Figure 1(b2), a 220 ms time window is available for IOS imaging without the effect of pupillary response to enable non-mydriatic ORG assessment of retinal photoreceptors.

Figure 3 illustrates spatiotemporal characterization of IOS distribution in the retina. Figure 3(a) shows the functional IOS image (Figure 2(c)) superimposed on the structural OCT (Figure 2(a)). This superimposed illustration confirmed that the fast photoreceptor-IOS is observed in the OS region, primarily distributed over OS boundaries connected with inner segment (IS) and retinal pigment epithelium (RPE). This observation was verified with two other human subjects with the same retinal stimulation and recording parameters (Figure 3(a2) and (a3)). Figure 3 (b) shows corresponding M-sequences, i.e. averaging IOS waveforms at each retinal depth, further confirming that the fast photoreceptor-IOSs attribute to the OS regions, predominantly distributed at the IS/OS and OS/RPE boundaries. For producing the M-sequence IOS map (Figure 3(b)), the IOS in each retinal depth was averaged. In other words, the IOS in horizontal direction of the B-scan image (Figure 3 (a)) was averaged. Each vertical line in Figure 3(b) corresponds to the whole 500 A-lines averaged recording at each time point. Figure 3(c) further confirms that rapid photoreceptor-IOS can be detected within 10 ms after the beginning of stimulus.

Discussion

In summary, technical feasibility of functional IOS imaging for objective, non-mydriatic ORG of retinal photoreceptors was demonstrated in awake humans. A custom designed OCT was constructed for functional IOS imaging of the retina. A pupil camera was used to verify that the pupillary response occurs ~220 ms after the onset of retinal stimulation (Figure 1(b1)). Therefore, a time window up to 220 ms provides the feasibility of non-mydriatic IOS imaging for objective ORG of photoreceptor function. The non-mydriatic imaging modality is essential for easy implementation of clinical applications.

Fast photoreceptor-IOS was consistently observed almost right away, before detectable pupillary response. Depth-resolved OCT verified the OS as the physical origin of fast photoreceptor-IOS. This observation is consistent to our previous animal studies with wild-type and transgenic mouse models.[26] Recently, light-evoked rapid optical path length changes within the cons OS were also reported in human studies[32,33] and increase of cone reflectance[36,37] in a few milliseconds. The fast photoreceptor-IOS is primarily confined at IS/OS and OS/RPE boundaries (Figure 3), supporting transient OS shrinkage due to phototransduction
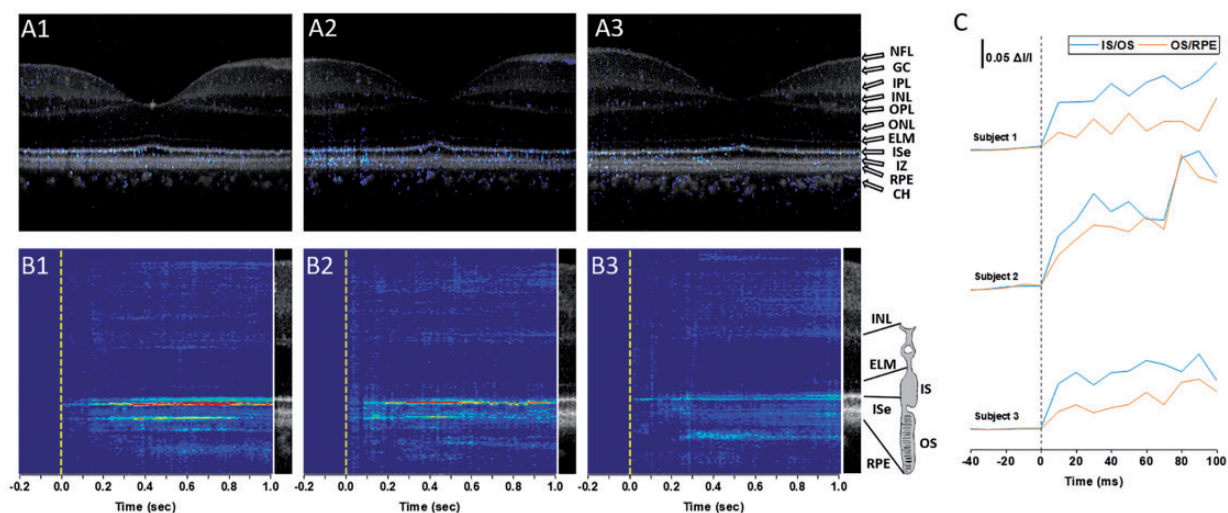
Figure 3. Spatiotemporal characterization of IOS changes in the retina. (a) Superimposed IOS maps over OCT B-scans. OCT and IOS images in (a1) correspond to the second frames of Figure 2(a2) and (c2), respectively. (a2) and (a3) are from two other human subjects. (b) M-sequence IOS maps show summed IOSs at each retinal depth. (b1)–(b3) correspond to the recordings in (a1)–(a3), respectively. (c) Averaging IOS activities at the IS/OS and OS/RPE boundary regions. Subjects 1–3 correspond to the recordings in (a1)–(a3), respectively. NFL: nerve fiber layer; GC: ganglion cells; IPL: inner plexiform layer; INL: inner nuclear layer; OPL: outer plexiform layer; ONL: outer nuclear layer; ELM: external limiting membrane; IS: inner segment; ISe: inner segment ellipsoid; OS: outer segment; IZ: interdigitation zone; RPE: retinal pigment epithelium; CH: choroid. (A color version of this figure is available in the online journal.)

process as the physiological mechanism of the fast photo-receptor-IOS.[38] The uneven IOS distribution in transverse direction was observed in the OS layer (Figures 2 and 3). This might result from the light sensitivity difference of individual photoreceptors. It is also known the rod and cone distribution is eccentricity dependent, relative to the fovea.[39,40] Further investigation, with variable stimulus light color and intensity controls, is required to characterize the spatiotemporal properties of the IOS in rod and cone photoreceptors. In animal study, transient OS conformational changes have been observed prior to the ERG a-wave which reflects the photoreceptor hyperpolarization.[41] Moreover, ERG a-wave could be reversibly blocked in low-sodium medium, but the light-evoked OS change was sustained in wide manner,[41] which supports that the signal source of the fast photoreceptor-IOS is not identical to that of ERG a-wave, cyclic guanosine monophosphate gated ion channel closure. Also, comparative IOS measurement in wild-type and retinal degeneration 10 mice revealed that fast photoreceptor-IOS arises before phosphodiesterase activation.[25] Therefore, the fast photoreceptor-IOS provides a unique biomarker for objective measurement of photoreceptor physiology.

AUTHORS' CONTRIBUTIONS

TS performed experiment, image analysis, and manuscript preparation; T-HK and GM contributed to image analysis; HK contributed to image preparation; and XY supervised the study and contributed to image analysis and manuscript preparation.

DECLARATION OF CONFLICTING INTERESTS

The author(s) declared no potential conflicts of interest with respect to the research, authorship, and/or publication of this article.

ORCID IDs

Taeyoon Son https://orcid.org/0000-0001-7273-5880
Tae-Hoon Kim https://orcid.org/0000-0002-4391-4860

REFERENCES

1. Holopigian K, Greenstein VC, Seiple W, Hood DC, Carr RE. Evidence for photoreceptor changes in patients with diabetic retinopathy. *Invest Ophthalmol Vis Sci* 1997;**38**:2355–65
2. McAnany JJ, Park JC. Cone photoreceptor dysfunction in Early-Stage diabetic retinopathy: association between the activation phase of cone phototransduction and the flicker electroretinogram. *Invest Ophthalmol Vis Sci* 2019;**60**:64–72
3. Berson EL, Gouras P, Gunkel RD. Rod responses in retinitis pigmentosa, dominantly inherited. *Arch Ophthalmol* 1968;**80**:58–67
4. Berson EL, Goldstein EB. Early receptor potential in dominantly inherited retinitis pigmentosa. *Arch Ophthalmol* 1970;**83**:412–20
5. Curcio CA, Medeiros NE, Millican CL. Photoreceptor loss in age-related macular degeneration. *Invest Ophthalmol Vis Sci* 1996;**37**:1236–49
6. Jackson GR, Owsley C, Curcio CA. Photoreceptor degeneration and dysfunction in aging and age-related maculopathy. *Ageing Res Rev* 2002;**1**:381–96
7. Sunness JS, Massof RW, Johnson MA, Bressler NM, Bressler SB, Fine SL. Diminished foveal sensitivity may predict the development of advanced age-related macular degeneration. *Ophthalmology* 1989;**96**:375–81
8. Seiple WH, Siegel IM, Carr RE, Mayron C. Evaluating macular function using the focal ERG. *Invest Ophthalmol Vis Sci* 1986;**27**:1123–30
9. Vaegan Billson F, Kemp S, Morgan M, Donnelley M, Montgomery P. Macular electroretinograms: their accuracy, specificity and implementation for clinical use. *Aust J Ophthalmol* 1984;**12**:359–72

10. Fish GE, Birch DG. The focal electroretinogram in the clinical assessment of macular disease. *Ophthalmology* 1989;**96**:109–14

11. Binns A, Margrain TH. Evaluation of retinal function using the dynamic focal cone ERG. *Ophthalmic Physiol Opt* 2005;**25**:492–500

12. Binns A, Margrain TH. Development of a technique for recording the focal rod ERG. *Ophthalmic Physiol Opt* 2006;**26**:71–9

13. Hood DC. Assessing retinal function with the multifocal technique. *Prog Retin Eye Res* 2000;**19**:607–46

14. Ball SL, Petry HM. Noninvasive assessment of retinal function in rats using multifocal electroretinography. *Invest Ophthalmol Vis Sci* 2000;**41**:610–7

15. Bizheva K, Pflug R, Hermann B, Povazay B, Sattmann H, Qiu P, Anger E, Reitsamer H, Popov S, Taylor JR, Unterhuber A, Ahnelt P, Drexler W. Optophysiology: depth-resolved probing of retinal physiology with functional ultrahigh-resolution optical coherence tomography. *Proc Natl Acad Sci U S A* 2006;**103**:5066–71

16. Yao X, Wang B. Intrinsic optical signal imaging of retinal physiology: a review. *J Biomed Opt* 2015;**20**:90901

17. Hunter JJ, Merigan WH, Schallek JB. Imaging retinal activity in the living eye. *Annu Rev Vis Sci* 2019;**5**:15–45

18. Michel-Villaz M, Brisson A, Chapron Y, Saibil H. Physical analysis of light-scattering changes in bovine photoreceptor membrane suspensions. *Biophys J* 1984;**46**:655–62

19. Harary HH, Brown JE, Pinto LH. Rapid light-induced changes in near infrared transmission of rods in *Bufo marinus*. *Science* 1978;**202**:1083–5

20. Kaplan MW. Concurrent birefringence and forward light-scattering measurements of flash-bleached rod outer segments. *J Opt Soc Am* 1981;**71**:1467–71

21. Kahlert M, Pepperberg DR, Hofmann KP. Effect of bleached rhodopsin on signal amplification in rod visual receptors. *Nature* 1990;**345**:537–9

22. Pepperberg DR, Kahlert M, Krause A, Hofmann KP. Photic modulation of a highly sensitive, near-infrared light-scattering signal recorded from intact retinal photoreceptors. *Proc Natl Acad Sci U S A* 1988;**85**:5531–5

23. Liebman PA, Jagger WS, Kaplan MW, Bargoot FG. Membrane structure changes in rod outer segments associated with rhodopsin bleaching. *Nature* 1974;**251**:31–6

24. Zhang QX, Zhang Y, Lu RW, Li YC, Pittler SJ, Kraft TW, Yao XC. Comparative intrinsic optical signal imaging of wild-type and mutant mouse retinas. *Opt Express* 2012;**20**:7646–54

25. Lu Y, Kim TH, Yao X. Comparative study of wild-type and rd10 mice reveals transient intrinsic optical signal response before phosphodiesterase activation in retinal photoreceptors. *Exp Biol Med (Maywood)* 2020;**245**:360–7

26. Yao X, Kim TH. Fast intrinsic optical signal correlates with activation phase of phototransduction in retinal photoreceptors. *Exp Biol Med (Maywood)* 2020;**245**:1087–95

27. Son T, Alam M, Toslak D, Wang B, Lu Y, Yao X. Functional optical coherence tomography of neurovascular coupling interactions in the retina. *J Biophotonics* 2018;**11**:e201800089

28. Wang B, Yao X. In vivo intrinsic optical signal imaging of mouse retinas. *Proc SPIE Int Soc Opt Eng* 2016;**9693**:96930H

29. Zhang Q, Lu R, Wang B, Messinger JD, Curcio CA, Yao X. Functional optical coherence tomography enables in vivo physiological assessment of retinal rod and cone photoreceptors. *Sci Rep* 2015;**5**:9595

30. Yao X, Son T, Kim TH, Lu Y. Functional optical coherence tomography of retinal photoreceptors. *Exp Biol Med (Maywood)* 2018;**243**:1256–64

31. Zhang PF, Zawadzki RJ, Goswami M, Nguyen PT, Yarov-Yarovoy V, Burns ME, Pugh EN. In vivo optophysiology reveals that G-protein activation triggers osmotic swelling and increased light scattering of rod photoreceptors. *Proc Natl Acad Sci U S A* 2017;**114**:E2937–46

32. Hillmann D, Spahr H, Pfaffle C, Sudkamp H, Franke G, Huttmann G. In vivo optical imaging of physiological responses to photostimulation in human photoreceptors. *Proc Natl Acad Sci U S A* 2016;**113**:13138–43

33. Zhang F, Kurokawa K, Lassoued A, Crowell JA, Miller DT. Cone photoreceptor classification in the living human eye from photostimulation-induced phase dynamics. *Proc Natl Acad Sci U S A* 2019;**116**:7951–6

34. Bergamin O, Kardon RH. Latency of the pupil light reflex: sample rate, stimulus intensity, and variation in normal subjects. *Invest Ophthalmol Vis Sci* 2003;**44**:1546–54

35. Kim TH, Wang B, Lu Y, Son T, Yao X. Functional optical coherence tomography enables in vivo optoretinography of photoreceptor dysfunction due to retinal degeneration. *Biomed Opt Express* 2020;**11**:5306–20

36. Jonnal RS, Rha J, Zhang Y, Cense B, Gao W, Miller DT. In vivo functional imaging of human cone photoreceptors. *Opt Express* 2007;**15**:16141–60

37. Bedggood P, Metha A. Optical imaging of human cone photoreceptors directly following the capture of light. *PLoS One* 2013;**8**:e79251

38. Lu Y, Benedetti J, Yao X. Light-induced length shrinkage of rod photoreceptor outer segments. *Transl Vis Sci Technol* 2018;**7**:29

39. Curcio CA, Sloan KR, Kalina RE, Hendrickson AE. Human photoreceptor topography. *J Comp Neurol* 1990;**292**:497–523

40. Curcio CA, Sloan KR Jr, Packer O, Hendrickson AE, Kalina RE. Distribution of cones in human and monkey retina: individual variability and radial asymmetry. *Science* 1987;**236**:579–82

41. Lu Y, Wang B, Pepperberg DR, Yao X. Light-evoked outer segment changes occur before the hyperpolarization of retinal photoreceptors. *Biomed Opt Express* 2017;**8**:38–47